Atmos. Chem. Phys., 14, 7859–7868, 2014
www.atmos-chem-phys.net/14/7859/2014/
doi:10.5194/acp-14-7859-2014

Atmospheric Chemistry and Physics
Open Access

Influence of cloud processing on CCN activation behaviour in the Thuringian Forest, Germany during HCCT-2010

S. Henning[1], K. Dieckmann[1], K. Ignatius[1], M. Schäfer[1,*], P. Zedler[1], E. Harris[2,], B. Sinha[2,3], D. van Pinxteren[1], S. Mertes[1], W. Birmili[1], M. Merkel[1], Z. Wu[1], A. Wiedensohler[1], H. Wex[1], H. Herrmann[1], and F. Stratmann[1]**

[1]Leibniz Institute for Tropospheric Research (TROPOS), 04318 Leipzig, Germany
[2]Particle Chemistry Department, Max Planck Institute for Chemistry, Hahn-Meitner-Weg 1, 55128 Mainz, Germany
[3]Department of Earth Sciences, Indian Institute of Science Education and Research Mohali, Sector 81, SAS Nagar, Manauli PO 140306, India
[*]now at: University of Leipzig, Faculty of Physics and Earth Sciences Leipzig Institute for Meteorology (LIM), Stephanstr. 3, 04103 Leipzig, Germany
[**]now at: Laboratory for Air Pollution and Environmental Technology, Swiss Federal Institute for Materials Science and Technology (EMPA), Überlandstrasse 128, 8600 Dübendorf, Switzerland

Correspondence to: S. Henning (henning@tropos.de)

Received: 19 December 2013 – Published in Atmos. Chem. Phys. Discuss.: 17 January 2014
Revised: 11 June 2014 – Accepted: 30 June 2014 – Published: 8 August 2014

Abstract. Within the framework of the "Hill Cap Cloud Thuringia 2010" (HCCT-2010) international cloud experiment, the influence of cloud processing on the activation properties of ambient aerosol particles was investigated. Particles were probed upwind and downwind of an orographic cap cloud on Mt Schmücke, which is part of a large mountain ridge in Thuringia, Germany. The activation properties of the particles were investigated by means of size-segregated cloud condensation nuclei (CCN) measurements at 3 to 4 different supersaturations. The observed CCN spectra together with the total particle spectra were used to calculate the hygroscopicity parameter κ for the upwind and downwind stations. The upwind and downwind critical diameters and κ values were then compared for defined cloud events (FCE) and non-cloud events (NCE). Cloud processing was found to increase the hygroscopicity of the aerosol particles significantly, with an average increase in κ of 50 %. Mass spectrometry analysis and isotopic analysis of the particles suggest that the observed increase in the hygroscopicity of the cloud-processed particles is due to an enrichment of sulfate and possibly also nitrate in the particle phase.

1 Introduction

Clouds are a key parameter in climate change prediction, due to their strong impact on the radiation processes in the atmosphere. However, the effect of aerosol particles on cloud formation, cloud glaciation and precipitation is still insufficiently quantified, and remains therefore one of the largest uncertainties in climate change predictions (Lohmann and Feichter, 2005; IPCC, 2013). Studying the interaction of aerosol and clouds under natural conditions is challenging due to the height as well as the spatial and temporal variability of clouds. Aside from extensive airplane, balloon or helicopter investigations of natural clouds (e.g. Krämer et al., 2013, p. 337), a well-established method for cloud investigation is to take advantage of natural clouds reaching the ground, allowing for ground-based experiments. This experimental design allows, for example, for the investigation of fog formation (e.g. Po Valley fog experiments; Svenningsson et al., 1992), advected stratiform clouds (e.g. Kleiner Feldberg, Wobrock et al., 1994), and also orographically triggered clouds (e.g. Schmücke, Herrmann et al., 2005).

One variation of the ground-based cloud experiments is a Lagrangian-type design. This involves locating several measurement stations in the predominant flow directions above a ridge, in order to probe

the air masses before, during and after cloud passage (e.g. Bower et al., 1999; Herrmann et al., 2005). The use of hill cap clouds as a natural flow-through reactor was for example realised successfully on Great Dun Fell (UK) (Bower et al., 1999; Choularton et al., 1997; Svenningsson et al., 1997), on the German mountain Kleiner Feldberg (Wobrock et al., 1994), during the cap cloud experiment of the 2nd Aerosol Characterisation Experiment (ACE-2 HILLCLOUD) at Teneriffe, Spain (Bower et al., 2000) and during FEBUKO (Field Investigations of Budgets and Conversions of Particle Phase Organics in Tropospheric Cloud Processes) at Mt. Schmücke (Herrmann et al., 2005).

The findings presented here were observed during the "Hill Cap Cloud Thuringia 2010" (HCCT-2010) cloud experiment, which was also conducted at the low mountain ridge around Mt Schmücke, where FEBUKO (Herrmann et al., 2005) took place. HCCT-2010 took place in September/October 2010 and dealt with several aspects of cloud microphysics and chemistry. An overview of HCCT-2010 is given in a companion paper in this special issue.

During the previous FEBUKO campaign, particle number size distribution measurements upwind (ambient) and on the summit (in-cloud: interstitial and residuals) were used to investigate the dependence of the scavenged aerosol fraction on the soluble volume fraction of the observed particles (Mertes et al., 2005a). In addition, at the upwind site, the hygroscopic properties were investigated (Lehmann et al., 2005) using Hygroscopic Tandem Differential Mobility Analyzer (HTDMA) measurements. Promising results were achieved concerning the dependence of the scavenged aerosol fraction on the soluble volume fraction of the particles. However, directly comparable activation or hygroscopicity measurements before and after the cloud passage were not carried out during FEBUKO. Aerosol processing was investigated by model simulation (Tilgner et al., 2005) and by comparing number size distribution upwind and downwind (Mertes et al., 2005b). Both studies show an effect on the aerosol size distribution in the size range of the activation diameter and an increase in aerosol number and mass.

The focus of the work presented here was to investigate the influence of cloud processing on the activation properties of aerosol particles. The interaction of particles with water can be described theoretically via Köhler theory (Köhler, 1936), which gives the equilibrium vapour pressure over an aqueous solution droplet. The maximum of the Köhler curve gives the critical supersaturation necessary for droplet activation. Classical Köhler theory needs several input parameters (e.g. molar weight of the particle substance, surface tension of the mixture) which are usually unknown for atmospheric particles. Therefore, one-parameter approximations were developed (e.g. Petters and Kreidenweis, 2007; Wex et al., 2007) which are applicable for the description of particle hygroscopic growth as well as activation properties. One-parameter approaches are also well suited as a simple measure to implement particle activation behaviour in modelling studies (e.g. Pringle et al., 2009).

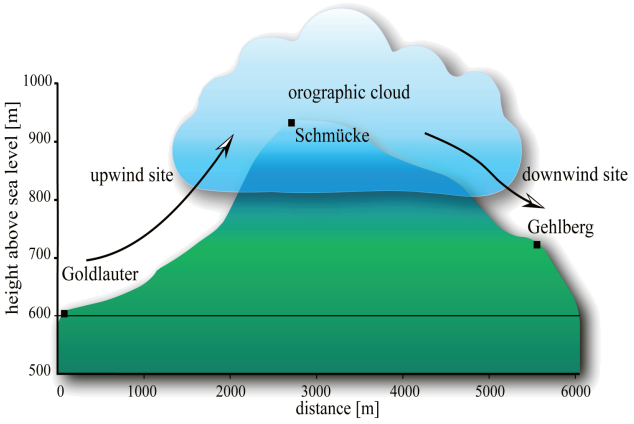

Figure 1. Sketch of the terrain of the HCCT experiment. For an approaching flow from the southwest, Goldlauter is the upwind station and Gehlberg the downwind station. This was the case for all defined full cloud events given in Table 1.

The results presented in this study are based on size-segregated CCN measurements at the upwind and downwind stations during periods of connected flow. The hygroscopicity parameter κ was deduced from the derived activation diameters. For selected non-precipitating cloud events on Mt Schmücke, the droplet activation properties at the upwind and downwind valley stations were compared, and the statistical significance of the findings was tested, in order to measure the influence of cloud passage on particle hygroscopicity. The same comparison between the upwind and downwind stations was also done for defined cloud-free periods as a control experiment.

2 Experimental design and setup

The experiments were conducted as part of the HCCT-2010 campaign, a Lagrangian-style experiment in which air parcels were probed at several locations during passage through an orographic cloud, focusing on the influence of cloud presence on the physical and chemical properties of the air parcel of interest (see companion paper for details). Briefly, measurements of meteorological parameters and physical and chemical aerosol and gas properties were conducted at three sites along the mountain ridge of the Thuringian Forest, Germany: one upwind station, the in-cloud mountain peak station on Mt Schmücke, and one downwind station (Fig. 1).

Time periods with optimal connected flow between the three stations were chosen by applying several different methods, e.g. shape of particle number size distribution, wind direction, wind speed and ozone concentration (Tilgner et al., 2014). These connected flow regimes were subdivided into

periods with a cap cloud present on Mt Schmücke and with the valley sites cloud free, so-called full cloud events (FCE, cf. Table 1), and cloud-free periods at all three stations, called non-cloud events (NCE). The FCE and NCE with CCN measurements available at the Goldlauter and Gehlberg stations are listed in Table 1 together with liquid water content (LWC), wind direction (wd) and wind speed (ws) on Mt Schmücke. LWC was measured by applying the Particulate Volume Monitor (PVM-100, Gerber Scientific Inc., Reston VA; Gerber, 1991). By coincidence, the FCE time periods with CCN data available at both valley stations had an approaching flow from a southwesterly direction, while for the NCE cases the flow approached from a northeasterly direction. This was taken into account in the data analysis and does not significantly affect the findings.

2.1 Measurement sites

The size-segregated CCN measurements took place at the upwind and downwind sites either side of Mt Schmücke, namely Gehlberg (GB) and Goldlauter (GL).

The Goldlauter (GL; 50°38′14″ N, 10°45′13″ E) valley station is situated on the southwestern slope of the Thuringian Forest mountain ridge. For FCE (southwesterly wind), this was the upwind station. That is, the air parcel was probed here before entering the cap cloud, and therefore represents the "pre-cloud" status of the aerosol. For NE_NCE (northeasterly wind), Goldlauter was the downwind station. All measurement equipment was placed inside an air-conditioned container. On top of the container a PM_{10} inlet followed by a self-regenerating diffusion drier was placed (Tuch et al., 2009), maintaining the relative humidity of the aerosol flow below 20 %. Inside the container – besides other instrumentation – a Mobility Particle Size Spectrometer (MPSS-type TROPOS; details of this instrument in Wiedensohler et al., 2012) was used to determine the particle number size distributions between 10 and 850 nm, and a Cloud Condensation Nucleus counter (CCNc, CCN-100, DMT Boulder, Roberts and Nenes, 2005) in combination with a differential mobility analyser (DMA) was used to measure CCN distributions between 25 and 300 nm.

The measurement equipment at the Gehlberg (GB; 50°40′21″ N, 10°47′34″ E) FCE downwind station was also placed inside an air-conditioned container. Here the PM_{10} inlet was followed by individual drier systems in front of the instruments instead of the self-regenerating diffusion drier applied in GL. This was the only difference in the size-segregated CCN measurement setup between both stations. Nafion driers (30 cm, TROPOS custom made) were placed in front of the TROPOS-type mobility particle size spectrometer and the DMA–CCNc, both of which kept the RH stable below 20 %. The data were corrected for the individual particle losses due to tubing and driers.

At these two sites and at Mt Schmücke (SM; 50°39′17″ N, 10°46′30″ E, 916 m a.s.l.), size-resolved (coarse and fine) particulate matter was collected for sulfur isotope analysis, with the in-cloud particulate separated into cloud droplet residual and interstitial fractions. In addition, at the upwind and downwind stations, SO_2 and H_2SO_4 gas and ultrafine particulate matter were collected. Combined scanning electron microscopy (SEM) and nano-scale secondary ion mass spectrometric (NanoSIMS) measurements were used to determine the isotopic composition of particulate sulfur samples ($\delta^{34}S$ fractionation factors) of the samples. Stable sulfur isotopes fractionate during reactions, so the isotopic composition of a product is not equal to the isotopic composition of the reactant. Using previous measurements of sulfur isotope fractionation factors characteristic of different oxidation pathways, e.g. oxidation by OH, H_2O_2 or transition metal ion catalysis (Harris et al., 2012, 2013a), the isotopic analyses made during HCCT-2010 allow dominant sulfate production pathways to be determined and resolved for different particle types, as described in Harris et al. (2014).

2.2 Size-segregated CCN measurements

The setup for the size-segregated activation measurements was identical at the upwind and downwind stations (Fig. 2), apart from the different drier types (cf. above). Downstream of the aerosol inlet and the drier unit, the $1\,L\,min^{-1}$ aerosol flow passed through a neutraliser to achieve the bipolar charge equilibrium (Wiedensohler, 1988). The DMA ran with an aerosol to sheath air flow of 1/10 to size-select aerosol particles based on electrical mobility, in order to achieve a quasi-monodisperse aerosol distribution. Multiply charged particles with larger sizes were also selected, for which the size and activation scans had to be corrected using the bipolar charge distribution. Downstream of the DMA, a flow of $0.5\,L\,min^{-1}$ particle-free air was added to the aerosol flow, and the total flow was divided between a particle counter ($1\,L\,min^{-1}$ working flow, CPC 3010, TSI Aachen Germany) and a cloud condensation nucleus counter ($0.5\,L\,min^{-1}$ working flow, CCNc, CCN-100, Boulder, USA). Measurements at the Goldlauter station were taken from 11 September 2010 to 20 October 2010, and in Gehlberg from 12 September 2010 to 20 October 2010, which is slightly shorter than the duration of the whole HCCT-2010 campaign.

The CCNc, a stream-wise thermal gradient cloud condensation nucleus counter (Roberts and Nenes, 2005), was applied to investigate supersaturation-dependent activation of the particles. In this instrument, the inlet flow is split into a particle-free sheath air flow, which is kept particle free via a filter, and an aerosol flow. The sheath air is humidified before entering the flow tube, and surrounds the aerosol at the centre line. The stream-wise temperature gradient applied in the flow tube determines the supersaturation to which the particles are exposed. The number of activated particles (N_{CCN}) is detected at the end of the flow tube with an optical counter. The ratio between the CCN number and the total

Table 1. Overview of all defined full cloud events (FCE) and non-cloud events (NE_NCE) for which CCN data are available at both valley stations.

	Start (CEST)	End (CEST)	LWC [g m^{-3}]	wd [°]	ws [m s^{-1}]
Cloud events					
FCE11.2	1 Oct 2010 20:50	2 Oct 2010 03:10	0.37	222.35	3.73
FCE11.3	2 Oct 2010 07:10	3 Oct 2010 00:30	0.35	223.98	6.58
FCE13.3	6 Oct 2010 06:50	7 Oct 2010 01:00	0.32	222.05	4.21
FCE22.0	19 Oct 2010 01:50	19 Oct 2010 09:00	0.29	226.76	5.96
FCE22.1	19 Oct 2010 21:10	20 Oct 2010 02:30	0.31	247.56	4.68
Non-cloud events					
NE_NCE0.1	7 Oct 2010 13:00	7 Oct 2010 18:50	–	49.40	1.27
NE_NCE0.2	8 Oct 2010 15:10	8 Oct 2010 18:30	–	59.70	2.24
NE_NCE0.3	9 Oct 2010 14:30	10 Oct 2010 09:30	–	68.88	4.67
NE_NCE0.4	10 Oct 2010 15:50	11 Oct 2010 03:30	–	51.36	5.66
NE_NCE0.5	11 Oct 2010 13:00	12 Oct 2010 04:40	–	51.61	5.72

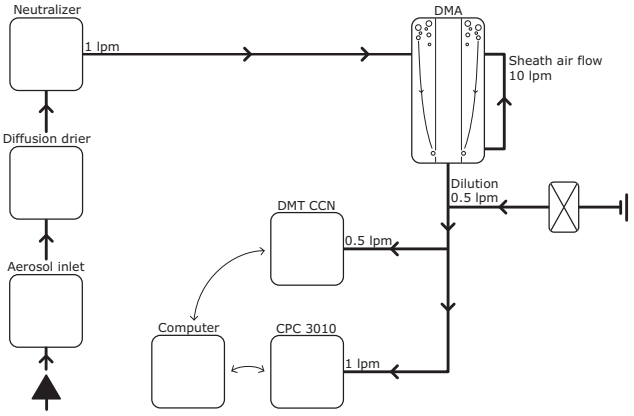

Figure 2. Setup for the size-segregated CCN measurements. The experimental setup was identical for the upwind and downwind sites.

particle number (N) gives the activated fraction (AF) of the particles. The CCNc was used to measure diameter scans for which the saturation is fixed, and the dry particle diameter is varied. In this study, we ran diameter scans for four fixed supersaturations (0.07, 0.1, 0.2, and 0.4 %). The critical particle diameter D_c, the diameter at which 50 % of the particles are activated at a particular supersaturation, is derived from such a diameter scan.

The supersaturation reached in the CCNc during the size-segregated CCN measurements was calibrated with ammonium sulfate particles. This was done by atomising an ammonium sulfate–water solution ($0.1\,g\,(NH_4)_2SO_4\,(300\,mL\,H_2O)^{-1}$), passing the resulting aerosol through a diffusion dryer, and injecting the dried particles into the CCN measurement setup (Fig. 2). The calibration procedure followed that described in Rose et al. (2008). In short, diameter scans were run at nominal supersaturations between 0.07 and 0.7 %, which relate to a certain temperature gradient in the flow tube of the CCNc. The AF were fitted by applying a Gaussian error function to the data:

$$\mathrm{AF} = \frac{a+b}{2}\left[1+\mathrm{erf}\left(\frac{D-D_c}{\sigma\sqrt{2}}\right)\right], \quad (1)$$

where a and b are the upper and lower limits for calculating critical diameters D_c at the set-nominal supersaturations. As $(NH_4)_2SO_4$ particles were used, the activation diameter is known, and the set temperature gradient in the instrument can be related to the effective supersaturation SS reached in the column. Repeated calibrations show an achievable accuracy in SS of 10 % (relative) at supersaturations above SS = 0.2 %, and δSS $\leq$ 0.02 % (absolute) at lower supersaturations (Gysel and Stratmann, 2013).

In the work presented here, we apply the single-parameter κ Köhler theory (Petters and Kreidenweis, 2007) to describe the hygroscopicity of the ambient particles. The hygroscopicity parameter κ is calculated in the following way (from Petters and Kreidenweis, 2007):

$$\kappa = \frac{4A^3}{27D_c^3\ln^2 \mathrm{SS}}, \quad (2)$$

with

$$A = \frac{4\sigma_{s/a}M_w}{RT\rho_w}. \quad (3)$$

The critical diameter is determined by fitting the AF scans to the error function (Eq. 1) analogously to the calibration procedure. The calibrated SS and measured D_c are inserted into Eq. (2) to calculate κ at fixed supersaturations for ambient particles. The error in the SS setpoint, especially at low

supersaturations, results in quite a large level of uncertainties in κ values. A critical diameter D_c of e.g. 200 nm at an SS of $0.07\% \pm 0.02\%$ corresponds to a κ range of 0.21 (SS = 0.09 %) < 0.35 < 0.94 (SS = 0.05 %). This is a critical point in working with κ, and has to be considered in the interpretation. This will be discussed more in Sect. 3.2.

2.3 Particle number size distribution measurements

In parallel to the CCN spectra, the particle number size distribution in the size range between 10 and 850 nm was measured at the Goldlauter and Gehlberg stations. The measurements were done with the above-mentioned mobility particle size spectrometers, which were connected to the same PM_{10} inlet as described above for the CCN measurements. Particle losses due to diffusion in the instrument and in the sampling lines have been corrected according to the method of "equivalent length" as described in Wiedensohler et al. (2012).

The CCN spectra have to be corrected for multiply charged particles, as the fitting of the AF with the error function is influenced by the appearance of a second step in the CCN spectra (Rose et al., 2008). This step is triggered by the fact that multiply charged large particles have the same electrical mobility diameter as singly charged smaller particles, and are thus falsely selected in the DMA. In the CCNc, however, they are activated at a lower supersaturation than the singly charged particles, and appear in the activated fraction vs. particle diameter curve as a first activation step at smaller diameters. How pronounced this first step is depends on the particle number size distribution, especially on the number of larger particles. The performed multiply charged correction is based on the measured number size distribution, and is described in detail in Deng et al. (2011): in brief, starting at larger sizes, the number of possible multiply charged particles at one size is calculated based on the charge equilibrium (Wiedensohler, 1988), and subtracted from the particle number at the corresponding smaller sizes. This is done for the whole N and N_{CCN} distribution from large to small particles.

3 Results and discussion

Ideally, a fixed time difference of 20 min would be applied to compare upwind and downwind measurements. That is, the measurement from the upwind station would be paired with a measurement from the downwind station, which was taken 20 min later. However, the set supersaturation should be the same at both stations for comparable measurements. Therefore, downwind data within 60 min of the upwind time stamp were included in the analysis. The number of activation measurements (n) per supersaturation (SS) for the matching time periods is given in Table 2.

3.1 Activation diameter and hygroscopicity parameter κ

The averaged values of the critical diameter (D_c), its standard deviation (σD_c) and the hygroscopicity parameter (κ) for each SS across all full cloud events (FCE) and non-cloud events (NCE) are given in Table 2. We merged all the FCE data and all the NCE data respectively in order to have a better statistical basis. During cloud events, D_c at the upwind station was observed to be larger than at the downwind station, with upwind values between 194.3 (SS = 0.07 %) and 122.9 nm (SS = 0.2 %) compared to downwind D_c between 173.9 (SS = 0.07 %) and 101.5 nm (SS = 0.2 %). Consequently, during cloud events, the calculated κ values at the upwind station (0.4, 0.42 and 0.19 for SS of 0.07, 0.1 and 0.2 %) were smaller than after cloud passage, where κ values of 0.54, 0.54 and 0.33 at SS of 0.07, 0.1 and 0.2 % were calculated. No significant changes in D_c and κ were observed for non-cloud events ($n = 55$, $p > 0.01$).

In Fig. 3a and b, the results are illustrated. The error bars were calculated by assuming a maximum absolute error in SS of ± 0.02 % for SS ≤ 0.2 %, by assuming a 10 % relative uncertainty for SS > 0.2 % (Gysel and Stratmann, 2013), and by applying Eq. (2) to calculate κ. Due to the nonlinear relation between SS and κ, the error bars are also asymmetric, and give the maximum uncertainty in κ. The increase in κ after the cloud passage in the FCE is obvious, whereas in the NCE the data fall together on the 1 : 1 line. However, the observed effect is within the measurement uncertainty – especially for the lower supersaturations. Therefore, we tested the statistical significance of the change in critical diameters (and thus κ values) between the stations during FCE and NCE, and re-estimated the uncertainty in κ by modelling the instrumental error in supersaturation by a Gaussian distribution.

3.2 Statistical analysis of the critical diameters and κ uncertainty estimation

We used statistical testing to determine if the change from upwind critical diameters $D_{c,up}$ to downwind critical diameters $D_{c,down}$ is significantly different between cloud and non-cloud events. This statistical testing scheme is known as "between-within" or "mixed" design, and it is analogous to the statistical experimental design in medicine called the "pre-post case control study", in which half of its patients are given medicine and the other half a placebo, and the patients are tested before and after the treatment. The experimental design is illustrated in Fig. 4. While testing, it is essential to take into account that the pre-measurement and post-measurement (upwind and downwind) points during the same day are paired, which accounts for variability between days and thus reduces noise. The simplest statistical test for a mixed design is called change score analysis (Oakes and Feldman, 2001), which is essentially a t test between Δ_{FCE}

Table 2. Mean critical diameter (D_c), standard deviation (σD_c) and hygroscopicity parameter (κ) for full cloud events (FCE: 11.2, 11.3, 13.3, 22.0 and 22.1) and non-cloud events (NE_NCE: 0.1, 0.2, 0.3, 0.4 and 0.5) at the Goldlauter and Gehlberg stations, separated by supersaturation (SS). N gives the number of cases where measurements could be compared between Goldlauter and Gehlberg.

			Upwind			Downwind		
Event	SS %	n	D_c nm	σD_c nm	κ^*	D_c nm	σD_c nm	κ
FCE	0.07	8	194.31	17.45	0.40	173.88	11.95	0.54
FCE	0.10	18	150.58	12.24	0.42	137.98	10.15	0.54
FCE	0.20	16	122.89	10.57	0.19	101.46	6.16	0.33
NCE	0.07	9	194.48	7.64	0.38	196.31	9.62	0.37
NCE	0.10	11	153.61	6.61	0.38	155.41	5.86	0.37
NCE	0.20	23	100.59	10.37	0.36	107.60	12.16	0.29
NCE	0.40	12	69.99	7.11	0.26	72.13	6.38	0.24

* Errors in κ are discussed in Sect. 3.2.

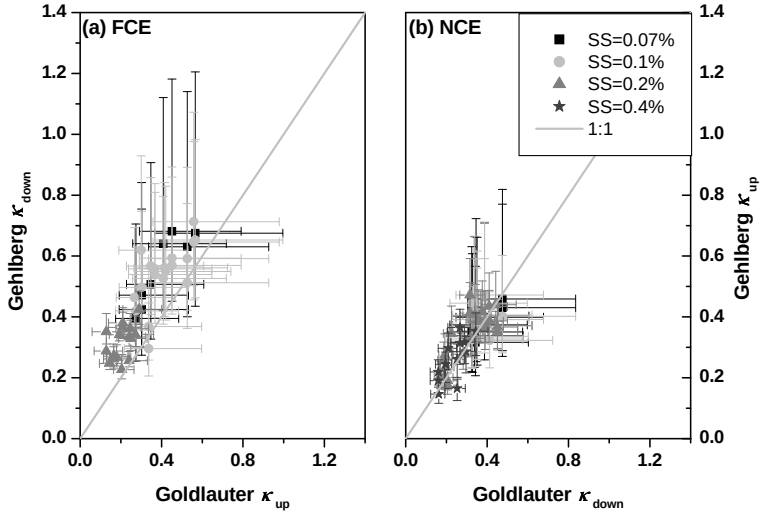

Figure 3. Hygroscopicity parameter κ compared for upwind and downwind stations during the full cloud events (FCE, left panel) and during non-cloud events (NCE, right panel). The error bars represent a maximum absolute error in SS of $\pm 0.02\,\%$ for SS $\leq 0.2\,\%$, and a 10 % relative uncertainty for SS $> 0.2\,\%$ (Gysel and Stratmann, 2013).

and Δ_{NCE} where $\Delta = D_{c,up} - D_{c,down}$. The null hypothesis was that there is no difference between FCE and NCE for $D_{c,down}$ with respect to $D_{c,up}$. A confidence of $p < 0.01$ was needed to reject the null hypothesis. The statistical analysis showed that for every supersaturation (0.07 %, 0.1 %, 0.2 %), the downwind critical diameters with respect to upwind diameters were significantly smaller during FCE than during NCE, with p values of 2.676×10^{-5}, 1.404×10^{-3} and 3.137×10^{-5} for the 0.07, 0.1 and 0.2 % supersaturations respectively. The critical diameter data sets for each supersaturation were tested separately. 0.4 % supersaturation was excluded from testing because there were no data for FCE periods.

We also checked with a t test that there is no significant difference between the FCE and NCE upwind critical diameters, in order to show that the differences in downwind critical diameters are caused by the cloud processes. As statisticians disagree on the correct statistical tests for mixed designs (Senn, 2006), we also applied the analysis of covariance (ANCOVA), assuming a linear model $D_{c,down} = \alpha + \text{cloudiness} + D_{c,up} + \epsilon$, where α is an intercept term, cloudiness is the parameter defining if the data point was measured during an FCE or NCE day, and ϵ is a Gaussian noise term. This test is used to investigate the statistical significance of the term cloudiness, using $D_{c,up}$ values as covariates. The results given by ANCOVA (not shown) are in good agreement with the p values obtained from the change score analysis.

Next, we estimated the uncertainty distribution of κ with Monte Carlo simulations. We have previously observed that the instrumental supersaturation error of the CCNc is

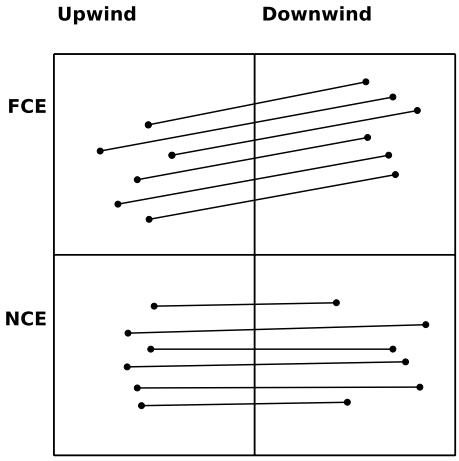

Figure 4. Schematic depiction of the experimental mixed design. The starting and end points of the black lines refer to the critical diameter data points.

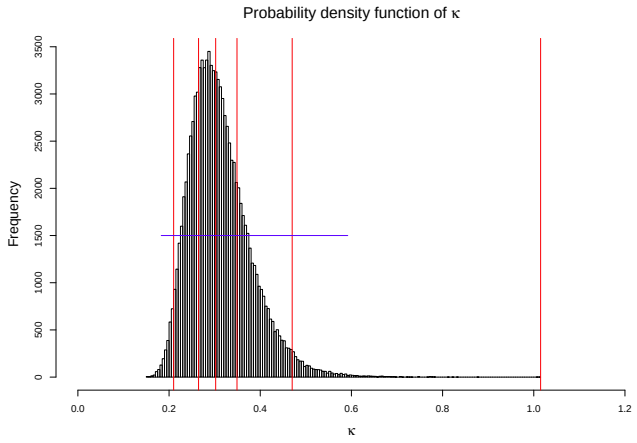

Figure 5. The uncertainty distribution of one κ measurement, produced by 100 000 Monte Carlo samples. Red vertical lines from left to right depict the 2.5, 25th, 50th, 75th, 97.5 and 100th percentiles; blue horizontal line illustrates the range of the original error bars.

Gaussian, with standard deviations of 0.00714 for 0.07, 0.1 and 0.2 % supersaturations and 0.01429 for 0.4 % supersaturation. These standard deviations are obtained from repeated calibration results showing that with a 95 % confidence level, the absolute uncertainty for supersaturations ≤ 0.2 % is ± 0.014 %, and for SS = 0.4 % the uncertainty is 0.027 %. The 95 % confidence level corresponds to 1.96σ, from which we can derive the aforementioned standard deviations. However, due to the nonlinear relationship between κ and the critical diameter, the uncertainty distribution of κ is non-Gaussian. The distribution of κ is simulated for each data point separately by drawing 100 000 random samples from a Gaussian supersaturation distribution ($\mu = 0.07, \sigma = 0.00714$) and by using Eq. (2). An example of a simulated κ distribution is presented in Fig. 5, showing the 2.5, 25th, 50th, 75th, 97.5 and 100th percentiles. All the analyses were done using R statistical software (R version 2.15.3, 2013).

By applying this statistical approach to the data, it is possible to present more realistic error bars. Using the maximum absolute error is a bad way of representing a Gaussian distribution, and since we know that the error in SS is Gaussian, the original error bars are a crude approximation. By assuming a Gaussian-distributed SS error, we are able to calculate the uncertainty distribution of κ (by Monte Carlo sampling), and from this distribution it is easy to calculate percentiles with which to represent error bars at the desired confidence level. Percentiles, e.g. 95 % confidence intervals, are a more correct way of representing the uncertainty in κ than the maximum absolute error. Figure 6a gives single κ values at the upwind station compared to the κ at the downwind station during FCE. The error bars presented in the figure are the 95 % confidence intervals calculated from the Monte Carlo simulations as explained above. All κ values derived for the downwind station are higher than those at the upwind station. The same analysis was again done for the NCE periods (Fig. 6b). Here, within error bars, the data of all SS fall onto the 1 : 1 line. This leads to the conclusion that we measured particles in NCE periods with the same hygroscopic properties at both the upwind and the downwind stations. The statistical test results support this conclusion. There is still considerable error in the κ values; however, the rigorous statistical analysis showed that the decrease in critical diameters due to cloud processing is significant. The results clearly demonstrate that the particle properties changed between upwind and downwind stations only when a hill cap cloud was present, leading to more hygroscopic aerosol particles downwind of the cloud.

3.3 Chemical in-cloud processing of the particles

Our findings can be explained by the enrichment of hygroscopic material in the particles during cloud presence. Assuming a chemical composition similar to the one given in Wu et al. (2013) for the upwind station, with a mass fraction of 40 % organic material and 30 % each of ammonium nitrate and ammonium sulfate, we can model an observed κ of e.g. 0.40 (compare Table 2). The measured increase in κ would during FCE translate to an increase in the mass fraction of 20 % in ammonium nitrate and ammonium sulfate between the upwind and downwind stations.

This estimate is supported by measurement results from other groups during HCCT-2010 who focused on the chemical and isotopic signatures of the particle populations; for example, sulfur isotope analysis of the particulate material was used to investigate the in-cloud production of sulfate. Combined gas-phase and single-particle measurements allowed the dominating sulfate production sources to be identified (Harris et al., 2014). Direct sulfate uptake, through dissolution of H_2SO_4 gas and scavenging of ultrafine particulate, as well as in-cloud aqueous SO_2 oxidation by H_2O_2,

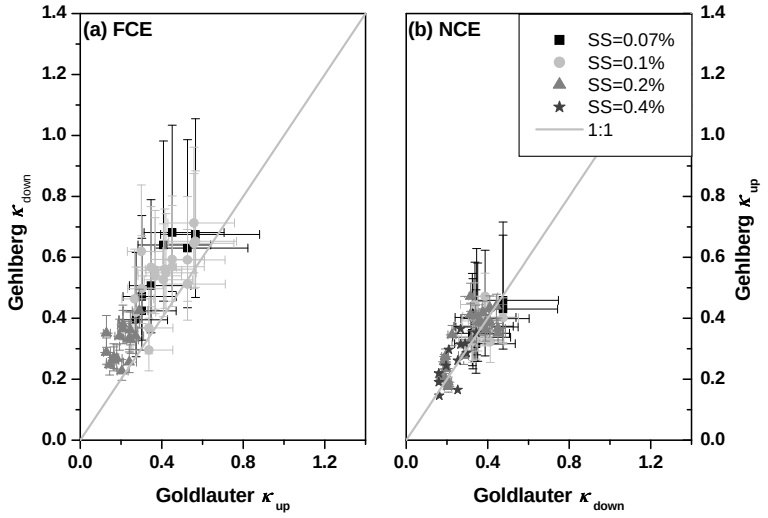

Figure 6. Hygroscopicity parameter κ compared for the upwind and downwind stations during the full cloud events (FCE, left panel) and non-cloud events (NCE, right panel), as given in Fig. 3. However, the error bars are the 2.5 and 97.5 % percentile limits for κ, produced by 100 000 Monte Carlo samples, and representing a confidence level of 95 %.

were found to be the most important sources for in-cloud addition of sulfate to mixed particles (the most common particle type during HCCT-2010), while in-cloud aqueous oxidation of SO_2 primarily catalysed by transition metal ions (Harris et al., 2013b) was most important for coarse mineral dust. The isotopic analyses showed that the sulfate content of particles increased following cloud processing during HCCT-2010 by > 10–40 % depending on particle type (cf. Table 5 in Harris et al., 2014).

Consistent with our results of increased hygroscopicity, both offline (impactor) and online (aerosol mass spectrometer) measurements of the chemical aerosol composition during HCCT often indicate an increased mass fraction of sulfate in aerosol particles after their passage through a cloud (van Pinxteren, Poulain, D'Anna, personal communications, 2013, data yet to be published in forthcoming companion papers of this special issue).

Mass spectrometric analysis of cloud residuals at the Schmücke in-cloud station showed an enhancement of nitrate in the cloud residuals compared to particles sampled under cloud-free conditions (Schneider et al., 2014). Additionally, a change in the mixing state was observed by single-particle mass spectrometry (Roth et al., 2014). The cloud residuals showed a higher fraction of particles mixed internally with sulfate and nitrate compared to the particles sampled under cloud-free conditions. These findings can be explained by an uptake of HNO_3 and sulfate production in the cloud droplets, resulting in an increased hygroscopicity after the cloud passage.

4 Summary and conclusions

In the ground-based HCCT-2010 cloud experiment, the activation diameters of aerosol particles were determined before and after passage across a hill. For cases with a proven connected flow, the activation properties of aerosol particles at the upwind and downwind stations were compared. For cases with a cap cloud on Mt Schmücke, a decrease in the critical diameter and a consequent increase of about 50 % in the hygroscopicity parameter κ were observed. In the cases with a connected flow between the valley stations and no cloud on the hill top, no change in the activation diameter was detected. The statistical significance of these findings was tested rigorously. All the κ values during cloud events were larger at the downwind station than at the upwind station, and the critical diameters were significantly smaller than during non-cloud days. Therefore, we conclude that in-cloud processes significantly increased CCN activity during all observed cloud events at HCCT-2010.

A possible explanation for the increased κ is the enrichment of more hygroscopic material during cloud processing, such as nitrates and sulfates. Particulate isotope measurements support our observations: dissolution of H_2SO_4 and scavenging of ultrafine particulate in the cloud as well as in-cloud aqueous SO_2 oxidation by H_2O_2 were identified as being the most important in-cloud sulfate addition processes for modifying CCN activity in the majority of the particles. Mass spectrometric measurements also corroborate the enrichment of soluble material in the particles in clouds: increased nitrate and a change in the mixing state were found in cloud residuals. Our measurements suggest that after cloud dissipation, the added hygroscopic material remains in the cloud residual aerosol particles.

Our results demonstrate the strong impact of in-cloud processing on the hygroscopic properties of potential CCN. Consideration of our findings in modelling studies will improve cloud representation substantially.

Acknowledgements. We would like to thank I. Huopaniemi for his advice concerning the statistical approach. The HCCT-2010 campaign was partially funded by the Deutsche Forschungsgemeinschaft (HE 3086/15-1). S. Mertes' participation was funded by DFG grant ME 3534/1-2.

Edited by: G. McFiggans

References

Bower, B. K. N., Choularton, T. W., Gallagher, M. W., Beswick, K. M., Flynn, M. J., Allen, A. G., Davison, B. M., James, J. D., Robertson, L., Harrison, R. M., Hewitt, C. N., Cape, J. N., McFadyen, G. G., Milford, C., Sutton, M. A., Martinsson, B. G., Frank, G., Swietlicki, E., Zhou, J., Berg, O. H., Mentes, B., Papaspiropoulos, G., Hansson, H. C., Leck, C., Kulmala, M., Aalto, P., Vakeva, M., Berner, A., Bizjak, M., Fuzzi, S., Laj, P., Facchini, M. C., Orsi, G., Ricci, L., Nielsen, M., Allan, B. J., Coe, H., McFiggans, G., Plane, J. M. C., Collett, J. L., Moore, K. F., and Sherman, D. E.: ACE-2 HILLCLOUD: an overview of the ACE-2 ground-based cloud experiment, Tellus B, 52, 750–778, 2000.

Bower, K. N., Choularton, T. W., Gallagher, M. W., Colvile, R. N., Beswick, K. M., Inglis, D. W. F., Bradbury, C., Martinsson, B. G., Swietlicki, E., Berg, O. H., Cederfelt, S. I., Frank, G., Zhou, J., Cape, J. N., Sutton, M. A., McFadyen, G. G., Milford, C., Birmili, W., Yuskiewicz, B. A., Wiedensohler, A., Stratmann, F., Wendisch, M., Berner, A., Ctyroky, P., Galambos, Z., Mesfin, S. H., Dusek, U., Dore, C. J., Lee, D. S., Pepler, S. A., Bizjak, M., and Divjak, B.: The Great Dun Fell experiment 1995: an overview, Atmos. Res., 50, 151–184, 1999.

Choularton, T. W., Colvile, R. N., Bower, K. N., Gallagher, M. W., Wells, M., Beswick, K. M., Arends, B. G., Mols, J. J., Kos, G. P. A., Fuzzi, S., Lind, J. A., Orsi, G., Facchini, M. C., Laj, P., Gieray, R., Wieser, P., Engelhardt, T., Berner, A., Kruisz, C., Moller, D., Acker, K., Wieprecht, W., Luttke, J., Levsen, K., Bizjak, M., Hansson, H. C., Cederfelt, S. I., Frank, G., Mentes, B., Martinsson, B., Orsini, D., Svenningsson, B., Swietlicki, E., Wiedensohler, A., Noone, K. J., Pahl, S., Winkler, P., Seyffer, E., Helas, G., Jaeschke, W., Georgii, H. W., Wobrock, W., Preiss, M., Maser, R., Schell, D., Dollard, G., Jones, B., Davies, T., Sedlak, D. L., David, M. M., Wendisch, M., Cape, J. N., Hargreaves, K. J., Sutton, M. A., StoretonWest, R. L., Fowler, D., Hallberg, A., Harrison, R. M., and Peak, J. D.: The Great Dun Fell cloud experiment 1993: an overview, Atmos. Environ., 31, 2393–2405, doi:10.1016/s1352-2310(96)00316-0, 1997.

Deng, Z. Z., Zhao, C. S., Ma, N., Liu, P. F., Ran, L., Xu, W. Y., Chen, J., Liang, Z., Liang, S., Huang, M. Y., Ma, X. C., Zhang, Q., Quan, J. N., Yan, P., Henning, S., Mildenberger, K., Sommerhage, E., Schäfer, M., Stratmann, F., and Wiedensohler, A.: Size-resolved and bulk activation properties of aerosols in the North China Plain, Atmos. Chem. Phys., 11, 3835–3846, doi:10.5194/acp-11-3835-2011, 2011.

Gerber, H.: Direct measurement of suspended particulate volume concentration and far-infrared extinction coefficient with a laser-diffraction instrument, Appl. Optics, 30, 4824–4831, 1991.

Gysel, M. and Stratmann, F.: WP3 – NA3: In-situ chemical, physical and optical properties of aerosols, Deliverable D3.11: Standardized protocol for CCN measurements, Tech. rep., http://www.actris.net/Publications/ACTRISQualityStandards/tabid/11271/language/en-GB/Default.aspx, 2013.

Harris, E., Sinha, B., Hoppe, P., Crowley, J. N., Ono, S., and Foley, S.: Sulfur isotope fractionation during oxidation of sulfur dioxide: gas-phase oxidation by OH radicals and aqueous oxidation by H_2O_2, O_3 and iron catalysis, Atmos. Chem. Phys., 12, 407–423, doi:10.5194/acp-12-407-2012, 2012.

Harris, E., Sinha, B., Hoppe, P., and Ono, S.: High-Precision Measurements of ^{33}S and ^{34}S Fractionation during SO_2 Oxidation Reveal Causes of Seasonality in SO_2 and Sulfate Isotopic Composition, Environ. Sci. Technol., 47, 12174–12183, doi:10.1021/es402824c, 2013a.

Harris, E., Sinha, B., van Pinxteren, D., Tilgner, A., Fomba, K. W., Schneider, J., Roth, A., Gnauk, T., Fahlbusch, B., Mertes, S., Lee, T., Collett, J., Foley, S., Borrmann, S., Hoppe, P., and Herrmann, H.: Enhanced role of transition metal ion catalysis during in-cloud oxidation of SO_2, Science, 340, 727–730, doi:10.1126/science.1230911, 2013b.

Harris, E., Sinha, B., Van Pinxteren, D., Schneider, J., Collett, J., Fahlbusch, B., Foley, S., Fomba, K. W., Gnauk, T., Lee, T., Mertes, S., Roth, A., Borrmann, S., Hoppe, P., and Herrmann, H.: In-cloud sulafte addition to single particles resolved with sulfur isotope analysis HCCT 2010, Atmos. Chem. Phys., 14, 4219–4235, doi:10.5194/acp-14-4219-2014, 2014.

Herrmann, H., Wolke, R., Muller, K., Bruggemann, E., Gnauk, T., Barzaghi, P., Mertes, S., Lehmann, K., Massling, A., Birmili, W., Wiedensohler, A., Wierprecht, W., Acker, K., Jaeschke, W., Kramberger, H., Svrcina, B., Bachmann, K., Collett, J. L., Galgon, D., Schwirn, K., Nowak, A., van Pinxteren, D., Plewka, A., Chemnitzer, R., Rud, C., Hofmann, D., Tilgner, A., Diehl, K., Heinold, B., Hinneburg, D., Knoth, O., Sehili, A. M., Simmel, M., Wurzler, S., Majdik, Z., Mauersberger, G., and Muller, F.: FEBUKO and MODMEP: field measurements and modelling of aerosol and cloud multiphase processes, Atmos. Environ., 39, 4169–4183, doi:10.1016/j.atmosenv.2005.02.004, 2005.

IPCC report 2013: Working Group I contribution to the AR5 on Climate Change 2013: the Physical Science Basis, Cambridge University Press, Cambridge, UK, New York, NY, USA, http://www.ipcc.ch/report/ar5/wg1, 2013.

Köhler, H.: The nucleus and the growth of hygroscopic droplets, T. Faraday Soc., 32, 1152–1161, 1936.

Krämer, M., Twohy, C. H., Hermann, M., Afchine, A., Dhaniyala, S., and Korolev, A.: Aerosol and cloud particle sampling, in: Airborne Measurements for Environmental Research: Methods and Instruments, edited by: Wendisch, M. and Brenguier, J. L., John Wiley & Sons, New York, Chichester, Weinheim, Brisbane, Singapore, Toronto, 2013.

Lehmann, K., Massling, A., Tilgner, A., Mertes, S., Galgon, D., and Wiedensohler, A.: Size-resolved soluble volume fractions of submicrometer particles in air masses of different character, Atmos.

Environ., 39, 4257–4266, doi:10.1016/j.atmosenv.2005.02.011, 2005.

Lohmann, U. and Feichter, J.: Global indirect aerosol effects: a review, Atmos. Chem. Phys., 5, 715–737, doi:10.5194/acp-5-715-2005, 2005.

Mertes, S., Lehmann, K., Nowak, A., Massling, A., and Wiedensohler, A.: Link between aerosol hygroscopic growth and droplet activation observed for hill-capped clouds at connected flow conditions during FEBUKO, Atmos. Environ., 39, 4247–4256, doi:10.1016/j.atmosenv.2005.02.010, 2005a.

Mertes, S., Galgon, D., Schwirn, K., Nowak, A., Lehmann, K., Massling, A., Wiedensohler, A., and Wieprecht, W.: Evolution of particle concentration and size distribution observed upwind, inside and downwind hill cap clouds at connected flow conditions during FEBUKO, Atmos. Environ., 39, 4233–4245, doi:10.1016/j.atmosenv.2005.02.009, 2005b.

Oakes, J. and Feldman, H.: Statistical power for nonequivalent pretest-posttest designs: the impact of Change-Score versus ANCOVA models, Evaluation Rev., 25, 3–28, doi:10.1177/0193841X0102500101, 2001.

Petters, M. D. and Kreidenweis, S. M.: A single parameter representation of hygroscopic growth and cloud condensation nucleus activity, Atmos. Chem. Phys., 7, 1961–1971, doi:10.5194/acp-7-1961-2007, 2007.

Pringle, K. J., Carslaw, K. S., Spracklen, D. V., Mann, G. M., and Chipperfield, M. P.: The relationship between aerosol and cloud drop number concentrations in a global aerosol microphysics model, Atmos. Chem. Phys., 9, 4131–4144, doi:10.5194/acp-9-4131-2009, 2009.

R version 2.15.3 (2013-03-01) – "Security Blanket" The R Foundation for Statistical Computing, ISBN 3-900051-07-0, 2013.

Roberts, G. C. and Nenes, A.: A continuous-flow streamwise thermal-gradient CCN chamber for atmospheric measurements, Aerosol Sci. Tech., 39, 206–221, 2005.

Rose, D., Gunthe, S. S., Mikhailov, E., Frank, G. P., Dusek, U., Andreae, M. O., and Pöschl, U.: Calibration and measurement uncertainties of a continuous-flow cloud condensation nuclei counter (DMT-CCNc): CCN activation of ammonium sulfate and sodium chloride aerosol particles in theory and experiment, Atmos. Chem. Phys., 8, 1153–1179, doi:10.5194/acp-8-1153-2008, 2008.

Roth, A., Schneider, J., Mertes, S., van Pinxteren, D., Herrmann, H., and Borrmann, S.: Observation of nitrate and sulfate increase in cloud residual particles sampled in orographic clouds by single particle mass spectrometry during HCCT2010, Atmos. Chem. Phys. Discuss., in preparation, 2014.

Schneider, J., Mertes, S., van Pinxteren, D., Tilgner, A., Herrmann, H., and Borrmann, S.: In situ mass spectrometric analysis of cloud residual composition in orographic clouds during HCCT2010: Evidence for uptake of nitric acid in cloud droplets, Atmos. Chem. Phys. Discuss., in preparation, 2014.

Senn, S.: Change from baseline and analysis of covariance revisited, Stat. Med., 25, 4334–4344, doi:10.1002/sim.2682, 2006.

Svenningsson, B., Hansson, H. C., Martinsson, B., Wiedensohler, A., Swietlicki, E., Cederfelt, S. I., Wendisch, M., Bower, K. N., Choularton, T. W., and Colvile, R. N.: Cloud droplet nucleation scavenging in relation to the size and hygroscopic behaviour of aerosol particles, Atmos. Environ., 31, 2463–2475, 1997.

Svenningsson, I. B., Hansson, H. C., Wiedensohler, A., Ogren, J. A., Noone, K. J., and Hallberg, A.: Hygroscopic growth of aerosol-particles in the Po Valley, Tellus B, 44, 556–569, 1992.

Tilgner, A., Majdik, Z., Sehili, A. M., Simmel, M., Wolke, R., and Herrmann, H.: SPACCIM: simulations of the multiphase chemistry occurring in the FEBUKO hill cap cloud experiments, Atmos. Environ., 39, 4389–4401, doi:10.1016/j.atmosenv.2005.02.028, 2005.

Tilgner, A., Schöne, L., Bräuer, P., van Pinxteren, D., Hoffmann, E., Spindler, G., Mertes, S., Birmili, W., Otto, R., Merkel, M., Weinhold, K., Wiedensohler, A., Deneke, H., Haunold, W., Engel, A., Wéber, A., and Herrmann, H.: Critical assessment of meteorological conditions and airflow connectivity during HCCT-2010, Atmos. Chem. Phys. Discuss., 14, 1861–1917, doi:10.5194/acpd-14-1861-2014, 2014.

Tuch, T. M., Haudek, A., Müller, T., Nowak, A., Wex, H., and Wiedensohler, A.: Design and performance of an automatic regenerating adsorption aerosol dryer for continuous operation at monitoring sites, Atmos. Meas. Tech., 2, 417–422, doi:10.5194/amt-2-417-2009, 2009.

Wex, H., Hennig, T., Salma, I., Ocskay, R., Kiselev, A., Henning, S., Massling, A., Wiedensohler, A., and Stratmann, F.: Hygroscopic growth and measured and modeled critical super-saturations of an atmospheric HULIS sample, Geophys. Res. Lett., 34, L02818, doi:10.1029/2006GL028260, 2007.

Wiedensohler, A.: An approximation of the bipolar charge-distribution for particles in the sub-micron size range, J. Aerosol Sci., 19, 387–389, 1988.

Wiedensohler, A., Birmili, W., Nowak, A., Sonntag, A., Weinhold, K., Merkel, M., Wehner, B., Tuch, T., Pfeifer, S., Fiebig, M., Fjäraa, A. M., Asmi, E., Sellegri, K., Depuy, R., Venzac, H., Villani, P., Laj, P., Aalto, P., Ogren, J. A., Swietlicki, E., Williams, P., Roldin, P., Quincey, P., Hüglin, C., Fierz-Schmidhauser, R., Gysel, M., Weingartner, E., Riccobono, F., Santos, S., Grüning, C., Faloon, K., Beddows, D., Harrison, R., Monahan, C., Jennings, S. G., O'Dowd, C. D., Marinoni, A., Horn, H.-G., Keck, L., Jiang, J., Scheckman, J., McMurry, P. H., Deng, Z., Zhao, C. S., Moerman, M., Henzing, B., de Leeuw, G., Löschau, G., and Bastian, S.: Mobility particle size spectrometers: harmonization of technical standards and data structure to facilitate high quality long-term observations of atmospheric particle number size distributions, Atmos. Meas. Tech., 5, 657–685, doi:10.5194/amt-5-657-2012, 2012.

Wobrock, W., Schell, D., Maser, R., Jaeschke, W., Georgii, H. W., Wieprecht, W., Arends, B. G., Mols, J. J., Kos, G. P. A., Fuzzi, S., Facchini, M. C., Orsi, G., Berner, A., Solly, I., Kruisz, C., Svenningsson, I. B., Wiedensohler, A., Hansson, H. C., Ogren, J. A., Noone, K. J., Hallberg, A., Pahl, S., Schneider, T., Winkler, P., Winiwarter, W., Colvile, R. N., Choularton, T. W., Flossmann, A. I., and Borrmann, S.: The Kleiner-Feldberg cloud experiment 1990 – an overview, J. Atmos. Chem., 19, 3–35, doi:10.1007/bf00696581, 1994.

Wu, Z. J., Poulain, L., Henning, S., Dieckmann, K., Birmili, W., Merkel, M., van Pinxteren, D., Spindler, G., Müller, K., Stratmann, F., Herrmann, H., and Wiedensohler, A.: Relating particle hygroscopicity and CCN activity to chemical composition during the HCCT-2010 field campaign, Atmos. Chem. Phys., 13, 7983–7996, doi:10.5194/acp-13-7983-2013, 2013.